

IMPEDANCE MATCHING CONTROLLER FOR AN INDUCTIVELY COUPLED PLASMA CHAMBER

L-type Matching Network Automatic Controller

Giorgio Bacelli, John V. Ringwood and Petar Iordanov

Department of Electronic Engineering, National University of Ireland, Maynooth, Ireland

Keywords: Automatic Impedance Matching, Matching Network, Impedance Sensor, Inductively Coupled Plasma.

Abstract: Plasma processing is used in a variety of industrial systems, including semiconductor manufacture (deposition and etching) and accurate control of the impedance matching network is vital if repeatable quality is to be achieved at the manufacturing process output. Typically, impedance matching networks employ series (tune) and parallel (load) capacitors to drive the reflection coefficient on the load side of the network to zero. The reflection coefficient is normally represented by real and imaginary parts, giving two variables to be controlled using the load and tune capacitors. The resulting problem is therefore a nonlinear, multivariable control problem. Current industrial impedance matching units employ simple single-loop proportional controllers, which take no account of interaction between individual channels and, in many cases, may fail to tune altogether, if the starting point is far away from the matching point. A hierarchical feedback controller is developed which, at the upper level, performs a single-loop tuning, but with the important addition of a variable sign feedback gain. When convergence to a region in the neighbourhood of the matching point is achieved, a dual single-loop controller takes over, which gives fine tuning of the matching network.

1 INTRODUCTION

The Basic Radio frequency Inductive System (BARIS) is an experimental inductively coupled plasma chamber used to study the closed-loop control of plasma states. Inductively coupled plasma is ignited by an electromagnetic field irradiated from an antenna connected to a Radio Frequency (RF) power supply. An Impedance Matching Unit (IMU) is used to match the impedance of the antenna to the impedance of the generator, in order to deliver the maximum power to the plasma. The IMU is composed of a matching network, a Phase and Magnitude Detector (PMD) and a controller that automatically tunes the matching network using the information supplied by the PMD. Each time plasma parameters or plasma state set-points are changed (i.e. RF power, pressure, gas mixture), the plasma impedance also changes. In addition, when the controller is tuning the matching network, the reflection coefficient is decreasing, therefore the power delivered to the plasma is increasing causing a variation of the plasma

states and, as a consequence, a variation of plasma impedance. The main issue regarding the existing driver circuitry associated with the original controller is the global convergence (Mazza, 1970), that is, if the initial conditions of the system are far away from the matching point, the controller may not be able to tune the matching network.

The automatic impedance matching problem has been solved using neural networks (Vai and Prasad, 1993), genetic algorithms (Thompson and Fidler, 2000) (Sun and J.K., 1997) (Sun and J.K., 1999), deterministic tuning algorithms with look-up tables (Moritz and Sun, 2001) and using adaptive systems (Parro and Pait, 2003) (Ida et al., 2004c) (Ida et al., 2004a) (De Mingo et al., 2004) (Ida et al., 2004b); nonlinear control systems have been also considered (Cottee, 2003). In all of the above mentioned cases, the load impedance is not affected by the matching conditions while, in the case studied (inductively coupled plasma discharges), the load impedance is varying during the matching process. In this paper a hierarchal structure controller has been designed; it is composed of

a higher level coarse controller that drives the system close to the matching point, and lower level feedback controller for the fine tuning. An impedance sensor has been also designed to supply more reliable measurements of the reflection coefficient to the controller.

2 BARIS IMPEDANCE MATCHING

The BARIS is an experimental plasma chamber, used to study plasma phenomenon for applications in semiconductor manufacturing, and generates an argon and oxygen plasma that is ignited by a 13.56MHz magnetic field irradiated from an antenna. The main parts that compose this device are the plasma discharge chamber, the RF power supply, the matching unit and the real time monitoring and control of the system.

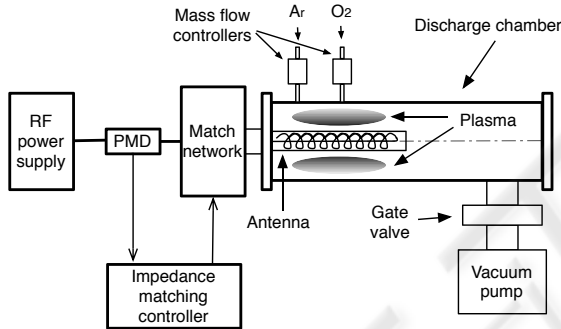


Figure 1: BARIS block diagram.

2.1 Plasma Discharge Chamber

The plasma discharge chamber is a stainless steel cylindrical vacuum chamber of internal diameter 200mm and length 900mm (Fig.1). The helical antenna is placed along the axis of the chamber, inside a sealed 50mm diameter quartz tube, in order to keep it outside of the vacuum region. The gasses are injected into the chamber by the mass flow controllers and are evacuated through the gate valve using a vacuum pump. The pressure at which the plasma is ignited is usually between 10mTorr and 100mTorr, and it is regulated by adjusting the position of the gate valve and the gas flows.

2.2 RF Power Supply

The RF power generator is the ACG-10B made by MKS Instruments, which can deliver a maximum of

1000W at a frequency of 13.56 MHz into a 50Ω load.

2.3 Plasma Process Monitoring and Control

The control of the plasma process is achieved using the Matlab xPC Target environment. This system is composed of two PCs, one running Windows XP (Host PC) and the other one running the real time xPC Target operative system (Target PC) as in Fig.2. The

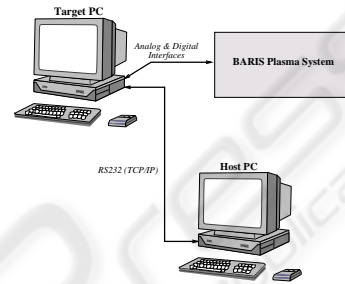


Figure 2: Matching network schematic.

Target PC is equipped with analog and digital interfaces in order to read data from sensors and control actuators and other devices. The role of the Host PC is to upload the software to be executed in real time by the Target PC, to start it, stop it and to monitor it while running using the RS-232 interface. This kind of configuration gives a considerable amount of computational power, allowing the implementation of complex control algorithm for the plasma process (Iordanov et al., 2006).

2.4 Matching Network

The matching network transforms the plasma load impedance (Z_{PL}) into the $Z_0 = 50\Omega$ characteristic impedance of the transmission line. It is a basic "L" configuration (Fig.3) characterized by eq.(1) and composed of "Load" (C_L) and "Tune" (C_T) variable capacitors, both driven by servomotors.

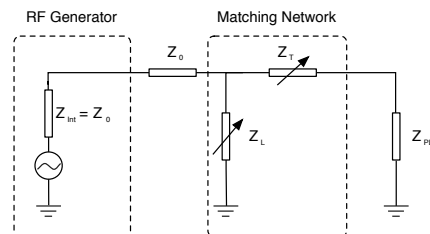


Figure 3: Matching network schematic.

$$Z_{PL} = \left[\frac{Z_0 Z_L}{Z_0 + Z_L} + Z_T \right]^*$$

$$= \left[\frac{Z_0}{(1 + \omega^2 Z_0^2 C_L^2)} + j \frac{(1 + \omega^2 Z_0^2 C_L (C_L + C_T))}{\omega C_T (1 + \omega^2 Z_0^2 C_L^2)} \right]^* \quad (1)$$

with:

$$Z_T = \frac{1}{j\omega C_T}, \quad Z_L = \frac{1}{j\omega C_L}, \quad \omega = 2\pi 13.56 \cdot 10^6 \text{ rad/s}$$

where [...] denotes complex conjugation and ω is the circular frequency.

3 SENSOR

The impedance sensor is based on the Analog Devices AD8302 phase and gain detector, which gives information about the amplitude ratio and the phase difference between two signals. The inputs of the circuit are two sinusoidal signals proportional to the voltage and the current waves in the power line respectively. By measuring the ratio between voltage and current and their phase difference, it is possible to calculate the impedance or the reflection coefficient. The impedance of a load connected in a transmission line is defined as (2),

$$Z_L = \frac{V_0}{I_0} \quad (2)$$

where V_0 and I_0 are the vectors of voltage and current respectively measured on the load and Z_L the load impedance. The last expression can be written using the vectors in the exponential form as in (3):

$$Z_L = \frac{V_0}{I_0} = \frac{|V_0| \cdot e^{j\theta_V}}{|I_0| \cdot e^{j\theta_I}} = \frac{|V_0|}{|I_0|} \cdot e^{j(\theta_V - \theta_I)} = G \cdot e^{\Delta\theta} \quad (3)$$

$$G = \frac{|V_0|}{|I_0|} \quad \Delta\theta = (\theta_V - \theta_I)$$

where G is the ratio between the voltage and the current magnitudes and $\Delta\theta$ is the phase difference between voltage and current waves. The impedance sensor provides two analog signals that are proportional to G and $\Delta\theta$. This device is divided in two parts, the "V-I Sensor" and the "Phase and Gain Sensor", each one enclosed in a shielded aluminum box in order to attenuate the effect of radio frequency disturbances (Fig.4). The former is connected along the high power transmission line, and supplies two signals proportional to the voltage and the current of the

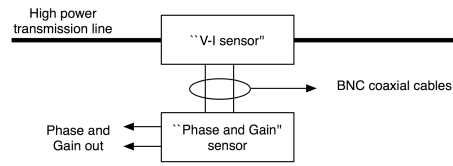


Figure 4: Block schematic of the impedance sensor.

main line. The "Phase and Gain Sensor" takes the output signals of the "V-I Sensor" and provides their phase difference and amplitude ratio. At the inputs of the AD8302 there are two integrated low pass filters (MINI-CIRCUITS SCLF-10.7) in order to remove the harmonics components.

4 CONTROLLER

The main property required of the controller is global convergence, that is the ability to drive the capacitors to the matching point from any starting condition. A model of the plasma impedance has been studied (Keville et al., 2006), but it is quite complicated, not suitable for the problem of the impedance matching because it is computationally demanding. The dynamics of the plasma process are stable and time invariant, in addition the part related to the RF power delivered P_D (Fig.5) is much faster than the dynamic of the matching unit, therefore it has been decided to consider the variation of the plasma impedance during the matching as a static disturbance. In this case the only dynamics terms considered in the system are due to the servomotors described by $G(s)$. Considering

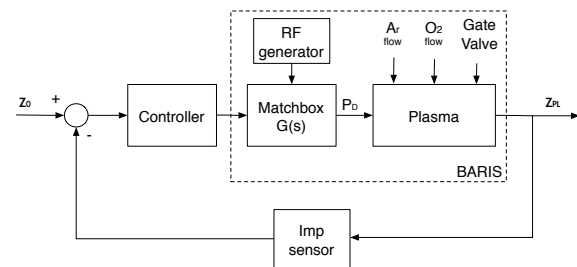


Figure 5: Block schematic of the BARIS.

the magnitude of the reflection coefficient $|\Gamma|$ as a function of the capacitors C_L and C_T , for a given value of the load impedance (Z_{PL}), using (1) is possible to plot the graph in Fig.6. The main characteristic of this function is that there is only one critical point corresponding to the global minimum, that is the matching point ($|\Gamma| = 0$). In this situation, the control problem

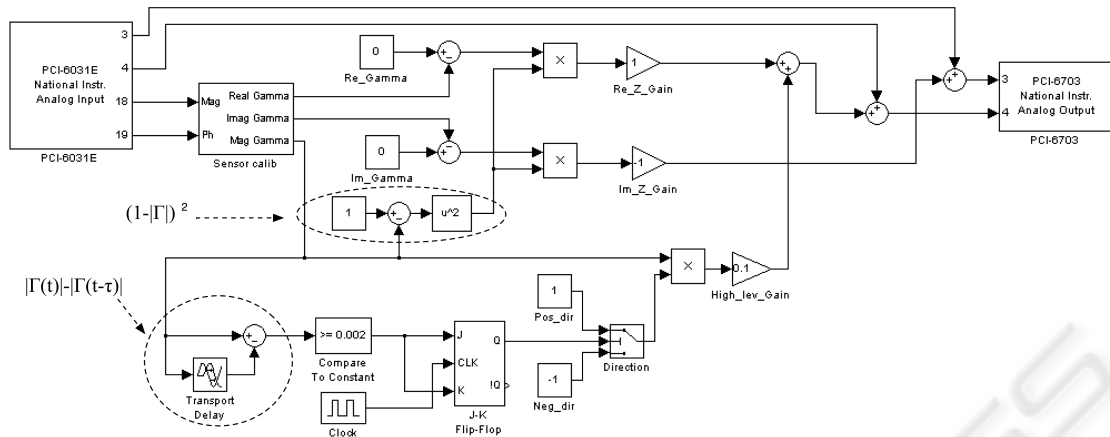


Figure 8: Simulink implementation of the hierarchical controller.

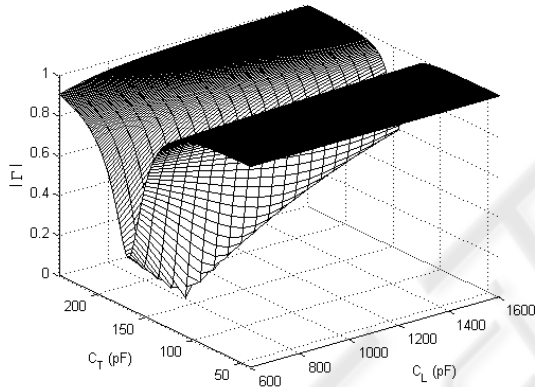


Figure 6: $|\Gamma|$ as function of (C_L, C_T) .

can be considered as a function minimization problem. A first possible approach can be to drive the capacitors in the opposite direction of the gradient of $|\Gamma|$, but the plasma impedance is variable and its value it is unknown, therefore it is not possible to calculate this vector. From Fig.6 is possible to see that $|\Gamma|$ is significantly more sensitive respect to C_T than C_L . We have decided to use a hierarchical structure composed of two parts: a coarse and a fine tune controller. The coarse controller brings the system close to the matching point, where the fine tune controller takes over and drives the capacitors to the final position. The coarse controller is based on an iterative minimization algorithm for $|\Gamma|$ respect to C_T , as in the flow chart in fig.7. At regular intervals of time δ it checks if the reflection coefficient and if it is increasing, it inverts the direction of movement of C_T . When

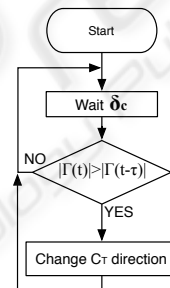


Figure 7: Iterative minimum search algorithm flow chart.

the system is approaching to the matching point there is a smooth transition between the coarse controller and the fine tune controller. The fine tune controller is a dual SISO proportional controller (Fig.9) in which C_L is driven by $Im[\Gamma]$ and C_T is driven by $Re[\Gamma]$.

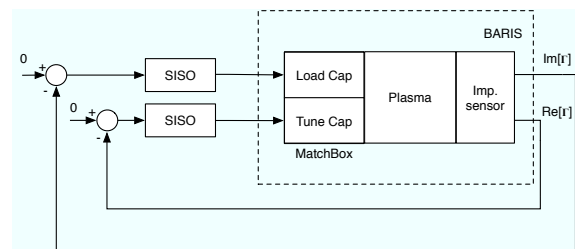


Figure 9: Block schematic of the fine tune controller.

4.1 Implementation

Fig.8 illustrates the Simulink implementation of the controller. The AD converter provides measurements

of G and $\Delta\theta$ at a sampling period of $\delta_f = 20mS$, which is also the sampling rate used by the fine tune controller. The coarse controller uses a sampling period of $\delta_c = 100mS$. $|\Gamma|$ is determined via eq (4) by the fine tune controller, allowing the delayed value of $|\Gamma(t - \tau)|$ to be available at the δ_c sampling instants ($\tau = 4\delta_f$).

$$\Gamma = \frac{Z_L - Z_0}{Z_L + Z_0} \quad (4)$$

The coarse controller checks the variation of the reflection coefficient $|\Gamma(t)| - |\Gamma(t - \tau)|$. If it is increasing, the J-K flip-flop inverts the direction of movement of C_T . Since the speed of C_T is proportional to $|\Gamma|$, the controller can be considered as a proportional controller. The gains of the fine tune SISO controllers are multiplied by $(1 - |\Gamma|)^2$ in order to reduce its effect in the non-convergence region, in which it tends to drive the capacitors in the wrong direction. In this way, when approaching to impedance matching condition, $|\Gamma|$ is decreasing and $(1 - |\Gamma|)^2$ is increasing, and there is a smooth transition from the coarse to the fine tune controller.

5 RESULTS

The controller has been tested both in simulation and in the BARIS chamber. The simulation has been performed using constant loads, and giving different starting positions for the capacitors. Figs.10 and 11 show that the system converges both when the initial conditions are close and far away to the matching point, that is the controller drives the capacitors in the right direction in order to minimize $|\Gamma|$. Fig.12

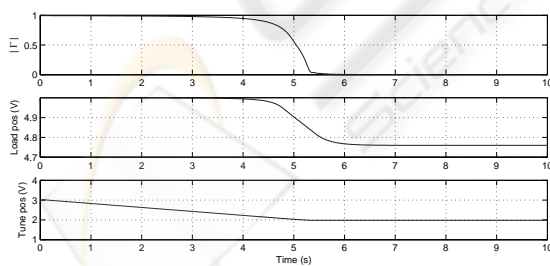


Figure 10: Simulation results with starting conditions close to the matching point.

shows the behavior of the system when the fine tune controller's gains are not multiplied by $(1 - |\Gamma|)^2$; for a starting condition far away from the matching point there is no convergence. In this case the coarse controller can't take over and the fine tune controller drives the capacitors in the wrong direction.

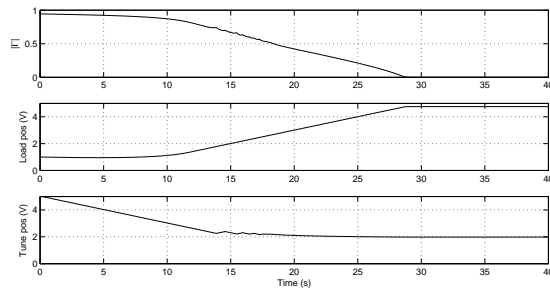


Figure 11: Hierarchical controller with starting conditions far away from the matching point.

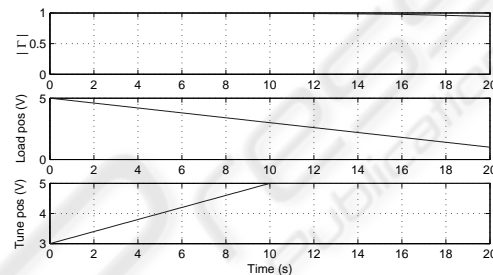


Figure 12: Hierarchical controller, with no fine tune controller gain attenuation.

The controller has been tested also in the BARIS system; this test has been performed using step functions for the plasma variables (RF power, pressure, A_r and O_2 flows). From the results of this test (Fig.13) it is possible to see that each time the plasma state changes, the controller tunes the matching network, minimizing the magnitude of the reflection coefficient $|\Gamma|$. In particular, mark A denotes a step in RF power, mark B denotes a step in the gate valve position, mark C denotes a step in O_2 flow and mark D denotes a step in A_r flow.

6 CONCLUSION

The hierarchical controller shows good performances regarding the convergence. Besides, it is computationally not demanding, giving the possibility to be implemented using a simple micro-controller. A multivariable controller, which observes the dependance of $Im[Z_{PL}]$ on both C_L and C_T was also designed, but requires an extensive look-up table and matrix inversion, which is in stark contrast to the attractive simplicity of the final controller presented above. The underlying principle of the controller is based only on the matching network structure, therefore it can be implemented also in other applications using a similar "L-type" matching network.

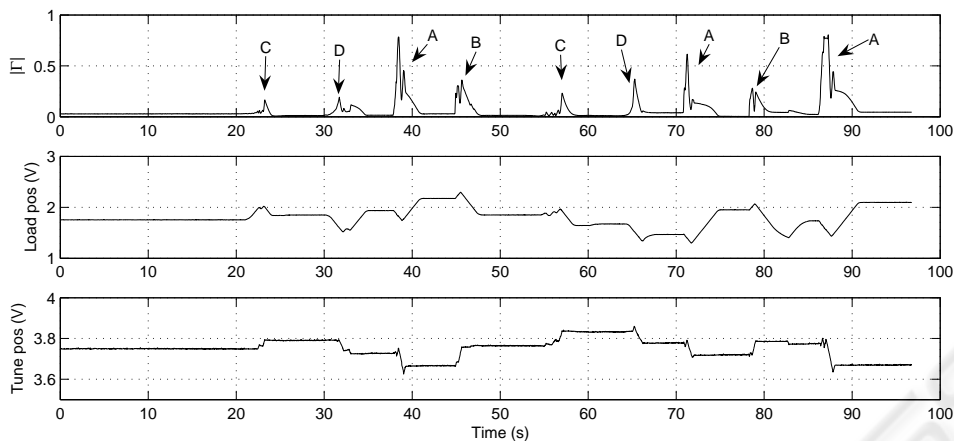


Figure 13: Experimental measurements in the BARIS.

ACKNOWLEDGEMENTS

The authors are grateful for the financial support of the Irish Research Council for Science Engineering and Technology (IRCSET) and INTEL Ireland Ltd.

REFERENCES

- Cottee, C.J.; Duncan, S. (2003). Design of matching circuit controllers for radio-frequency heating. *IEEE Transactions on Control Systems Technology*, 11(1):91–100.
- De Mingo, J., Valdovinos, A., Crespo, A., Navarro, D., and Garcia, P. (2004). An RF electronically controlled impedance tuning network design and its application to an antenna input impedance automatic matching system. *IEEE Transactions on Microwave Theory and Techniques*, 52(2):489–497.
- Ida, I., Takada, J., Toda, T., and Oishi, Y. (2004a). An adaptive impedance matching system and considerations for a better performance. *IEEE 5th International Symposium on Multi-Dimensional Mobile Communications Proceedings*, 2:563–567.
- Ida, I., Takada, J., Toda, T., and Oishi, Y. (2004b). An adaptive impedance matching system and its application to mobile antennas. *IEEE Region 10 Conference*, 3:543–546.
- Ida, I., Takada, J., Toda, T., and Oishi, Y. (2004c). An adaptive impedance matching system for mobile communication antennas. *IEEE Antennas and Propagation Society International Symposium*, 3:3203–3206.
- Iordanov, P., Keville, B., Ringwood, J., and Doherty, S. (2006). On the closed-loop control of an argon plasma process. *Irish Signals and Systems Conference*.
- Keville, B., Iordanov, P., Ringwood, J., Doherty, S., Faulkner, R., Soberon, F., and McCarter, A. (2006). On the modeling and closed loop control of an inductively coupled plasma chamber. *IFAC Workshop on Advanced Process Control for Semiconductor Manufacturing*.
- Mazza, N. (1970). Automatic impedance matching system for RF sputtering. *IBM Journal of Research and Development*, 14(2).
- Moritz, J. and Sun, Y. (2001). Frequency agile antenna tuning and matching. *IEE Eighth International Conference on HF Radio Systems and Techniques*, 148:177–182.
- Parro, V. and Pait, F. (2003). Design of an automatic impedance matching system for industrial continuous microwave ovens. *Sociedade Brasileira de Microondas Optoeletronica/IEEE Microwave and Optoelectronics Conference*, 2:20–23.
- Sun, Y. and J.K., F. (1997). Component values ranges of tunable impedance matching networks in rf communications systems. *IEE HF Radio Systems and Techniques*, 441.
- Sun, Y. and J.K., F. (1999). Antenna impedance matching using genetic algorithms. *IEE National Conference on Antennas and Propagation*, 441:31–36.
- Thompson, M. and Fidler, J. (2000). Application of the genetic algorithm and simulated annealing to LC filter tuning. *IEE Circuits, Devices and Systems*, 474(2):169–174.
- Vai, M. and Prasad, S. (1993). Automatic impedance matching with a neural network. *IEEE Microwave and Guided Wave Letters*, 3(10).